Physica B 406 (2011) 4245–4248

Contents lists available at SciVerse ScienceDirect

Physica B

journal homepage: www.elsevier.com/locate/physb

Half-metallicity and magnetic properties of half-Heusler type Mn_2Sn: Ab initio predictions

H.Z. Luo [a,b,*], G.D. Liu [a], F.B. Meng [a], W.H. Wang [b], G.H. Wu [b], X.X. Zhu [c], C.B. Jiang [c]

[a] School of Material Science and Engineering, Hebei University of Technology, Tianjin 300130, PR China
[b] Beijing National Laboratory for Condensed Matter Physics, Institute of Physics, Chinese Academy of Sciences, Beijing 100190, PR China
[c] Beijing University of Aeronautics and Astronautics, Beijing 100191, PR China

ARTICLE INFO

Article history:
Received 20 May 2011
Received in revised form
7 August 2011
Accepted 8 August 2011
Available online 11 August 2011

Keywords:
Heusler alloy
Band structure
Half-metal

ABSTRACT

Ab initio calculations have been carried out to investigate the electronic structure and magnetism of the compound Mn_2Sn with the bcc half-Heusler structure. For the equilibrium lattice parameter 5.69 Å, Mn_2Sn is predicted to be a half-metallic fully compensated ferrimagnet (also called half-metallic antiferromagnet) with zero total spin moment. This zero moment agrees well with the Slater–Pauling curve and mainly comes from the compensated Mn (A) and Mn (B) spin moments in antiparallel configuration. The half-metallicity of Mn_2Sn is stable in a wide lattice-parameter range from 5.6 Å to 5.9 Å. Upon contraction of the lattice, a transition from half-metallicity to semimetallicity is observed.

1. Introduction

In the recent years, with the development of spintronic devices, materials with complete spin polarization at the Fermi level E_F have attracted much attention because they are of great interest for scientific research and industrial applications [1–3]. These materials have an energy gap in one spin band at E_F whereas the other spin band overlaps with the Fermi level and shows metallic character, which results in a complete spin polarization of the conduction electrons at E_F. Therefore, these materials are also called half-metallic ferromagnets (HMFs). They have a 100% spin-polarized current and can be used as spin injectors for magnetic random-access memories and other spin-dependant devices [1,2].

Besides experimental studies, also first-principles electronic-structure calculations play an important role in the prediction of half-metals and their integration into real devices [4]. The Heusler alloys form a large family in half-metallic materials. They usually have high Curie temperatures and can be easily prepared as thin films. All this makes half-metallic Heusler alloys good candidates for spintronic materials. In fact the first predicted half-metal was NiMnSb, a half-Heusler alloy [1]. Heusler alloys can be divided into full-Heusler alloys and half-Heusler alloys by the number of atoms in one unit cell; the chemical formulae for them are X_2YZ and XYZ, respectively, where X and Y are transition-metal elements and Z is the main-group element. In the half-Heusler alloys, one X atom is replaced by a vacant site.

In the studies of half-metallic Heusler alloys, compounds with a ferrimagnetic structure are rather interesting. In these half-metallic ferrimagnets the transition-metal atoms at different sites in the unit cell have antiparallel spin moments, which compensate each other. It is known that the total spin moments of the half-metals follow the Slater–Pauling (S–P) curve, which is $M_t=Z_t-24$ for full-Heusler alloys and $M_t=Z_t-18$ for half-Heusler alloys, where M_t is the total magnetic moment per formula unit (f.u.) and Z_t the total number of valence electrons [4]. So it may be expected that in the half-metallic ferrimagnets with 24 (full-Heusler alloys) or 18 (half-Heusler alloys) valence electrons, the magnetic moments of different atoms can completely compensate each other, resulting in a zero total moment. This kind of half-metal is also called half-metallic antiferromagnet (HMA) or half-metallic fully compensated ferrimagnet (HMFCF) [5,6]. Because of its weak magnetic moment, a HMFCF itself will create a very small external magnetic field, which is supposed to have advantages in many technical applications [6].

Till now, most studies on HMFCFs are theoretical and focus on full-Heusler alloys. Wurmehl et al. [6] have predicted Mn_3Ga to be a HMFCF, in which the compensated magnetic moments mainly come from the spin moments of Mn at different crystallographic sites. Also Cr_2MnZ (Z=P, As, Sb, Bi) and Cr_2CoAl have been predicted to be HMFCFs [7,8]. Galanakis et al. [9] have reported HMFCF properties of Mn_2VAl and Mn_2VSi upon substitution of Co

* Corresponding author at: School of Material Science and Engineering, Hebei University of Technology, Tianjin 300130, PR China. Tel.: +86 10 8264 9247; fax: +86 10 6256 9068.
E-mail addresses: hongzhi_luo@yahoo.com.cn, luo_hongzhi@163.com (H.Z. Luo).

0921-4526/$ - see front matter © 2011 Elsevier B.V. All rights reserved.
doi:10.1016/j.physb.2011.08.020

for Mn, the compensated moments mainly coming from the antiparallelly aligned Mn and Co moments. Of the half-Heusler alloys, only MnCrSb has been reported by van Leuken and De Groot [5]. Therefore it is interesting to investigate and synthesize more HMFCFs.

From the studies above, we see that Mn atoms play an important role in the formation of HMFCFs. The Mn moment tends to be antiparallel to the spin moments of other atoms, which is necessary to obtain the fully compensated total moment in HMFCFs. In this paper, we investigate the electronic structure and magnetism of the half-Heusler alloy Mn_2Sn with 18 valence electrons and report its half-metallic properties.

It should be emphasized that Mn_2Sn crystallizes in the hcp $B8_2$-type structure [10] and not in the bcc $L2_1$ phase for which the present calculations have been carried out. However, with the present technological developments, it is possible to grow metastable thin films with structures that do not exist in bulk form. Therefore, the bcc Mn_2Sn reported in this study may eventually be prepared by molecular-beam epitaxy or a similar method. In spintronic devices, half-metals are also used as thin films. Unlike the other ternary half-Heusler alloys Mn_2Sn is a binary one, studies on which can help to explore new functional materials in this kind of alloys. Recently, similar calculations have also been performed by Fujii et al. on FeCrZ and MnYZ [11].

2. Computational method

The electronic structure was calculated by means of the CASETP code based on the pseudopotential method with a plane-wave basis set [12,13]. The interactions between the atomic core and the valence electrons were described by the ultrasoft pseudopotential. [14] The electronic exchange–correlation energy was treated under the local-density approximation (LDA) [15,16]. A plane-wave basis set cut-off of 500 eV was used in all cases and a mesh of $16\times16\times16$ k-points was employed for the Brillouin zone integrations. These parameters ensured good convergence of the total energy. The convergence tolerance for the calculations was selected as 1×10^{-6} eV/atom. The calculations were performed based on the theoretical equilibrium lattice parameters.

The half-Heusler alloy XYZ crystallizes in the body-centered cubic (bcc) structure with one formula unit per primitive cell. The space group is $F\bar{4}3m$. In this study, Mn represents the X and Y atoms and Sn represents the Z atom. Half-Heusler alloys in the conventionally stable structure of the Y and Z atoms are located at A (0 0 0) and C (1/2 1/2 1/2) sites and form the rock salt structure while the X atom is located in the octahedrally coordinated pocket at the cube-center site B (1/4 1/4 1/4), leaving the other site D (3/4 3/4 3/4) unoccupied [17,18].

3. Results and discussion

To determine the lattice parameter of Mn_2Sn, we performed structural optimizations on it for both the non-magnetic (PM) and the ferromagnetic (FM) states. The calculated equilibrium lattice parameter is 5.69 Å for Mn_2Sn. This lattice parameter is somewhat smaller than the result of Fujii et al. (6.098 Å) [11] and may be related to the so-called LDA overbinding effect [19].

Fig. 1 presents the total and partial densities of states (DOS) of Mn_2Sn at the equilibrium lattice parameter. Mn_2Sn has 18 valence electrons, which tend to occupy the majority and minority spin band equally. So there are nine electrons in both spin bands of Mn_2Sn, which makes it difficult to identify the majority and minority spin states simply by the number of electrons in them. In Fig. 1, we choose the spin states with the energy gap

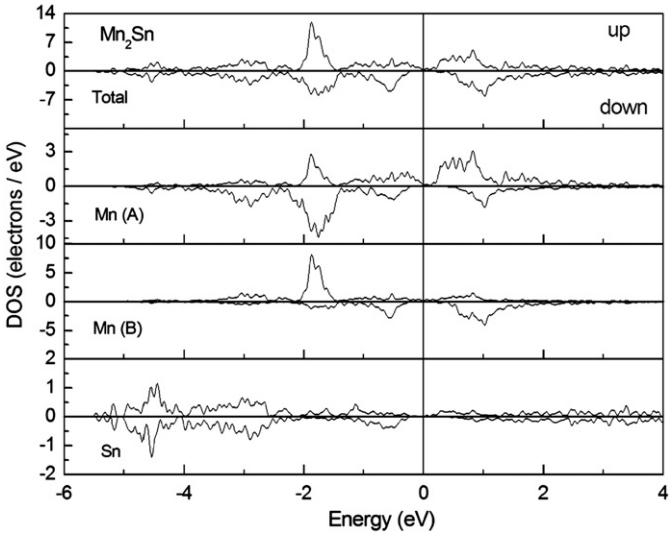

Fig. 1. Calculated spin-projected total and partial DOS of Mn_2Sn.

around E_F to be the minority spin states. There are no states in this minority energy gap. However, in the majority spin states, E_F is located in a low-DOS region. All this results in a 100% spin polarization of the conduction electrons at E_F, so that Mn_2Sn is a half-metal at the equilibrium lattice parameter.

In Fig. 1, a clear magnetic splitting is observed in the total DOS though the 18 valence electrons occupy the spin-up and -down band equally. The magnetic splitting mainly comes from the PDOS of Mn atoms at the A and B sites. In Fig. 1, it can be seen that the PDOS of Mn (A) and Mn (B) have opposite configuration. In the majority states of Mn (B) the bonding peak is far below the Fermi level and occupied and, in the minority states, the antibonding peak is far above E_F and unoccupied. In contrast, for the PDOS of Mn (A), the unoccupied antibonding peak is far above E_F in the majority spin and the occupied minority bonding peak is far below E_F. Therefore the contributions to the total DOS from Mn (A) and Mn (B) are opposite to each other, corresponding to an antiparallel alignment of their spin moments [6]. In Ref. [11], antiparallel alignment between the Mn moments of Mn_2Sn has also been reported.

From the PDOS it can also be seen that the structure of the half-metallic gap is mainly determined by the DOS of Mn (A) and Mn (B). As discussed above, the majority states of Mn (B) are basically occupied with a high antibonding peak below E_F. These states are hybridized with Mn (A) d states, forming a broad d band. In the minority spin band, exchange splitting shifts the antibonding peak of Mn (B) to higher energy above E_F and forms an energy gap between the bonding and antibonding peaks. So, similar to other half-Heusler alloys [20], the origin of the half-metallic gap in Mn_2Sn can be attributed to strong hybridization between the d states of the Mn atoms. The Fermi level is located between the bonding t_{2g} orbitals and antibonding e_g orbitals.

The calculated total spin moment for Mn_2Sn is 0.001 μ_B/f.u., which agrees well with the Slater–Pauling curve. There are 18 valence electrons in Mn_2Sn, which equally occupy the majority and minority spin bands, so that a zero total spin moment results ($M_t=Z_t-18$). In Mn_2Sn, there are mainly the antiparallel Mn spin moments that lead to the zero total moment. The partial moments are $-2.22\mu_B$, $2.24\mu_B$ and $-0.02\mu_B$ for Mn (A), Mn (B) and Sn, respectively. In Ref. [11], the Mn (A) and Mn (B) moments are $-3.16\mu_B$ and $3.44\mu_B$, respectively. These larger moments can be traced back to the larger equilibrium lattice parameter in Ref. [11], which enhances the localization of Mn d states and increases the spin moments.

According to a study on Cr_2MnZ a small change of the lattice parameter may shift E_F with respect to the half-metallic gap, which clearly affects the half-metallicity as well as the transport properties [7]. Meanwhile half-metals are usually prepared as thin films for application in spintronic devices, in which the lattice constant of the material is strongly influenced by the lattice of the substrate. All this makes it necessary to consider the influence of lattice distortion on half-metallicity. In the present paper, we have studied the electronic structure of Mn_2Sn with uniform lattice distortion from 5.5 Å to 6.1 Å (−3.5% −6% changes with respect to the equilibrium lattice parameter).

In Fig. 2, we present the energy bands of Mn_2Sn for different lattice parameters. At the equilibrium lattice parameter (5.69 Å), the energy bands show clear half-metallic character. In the majority spin band, the Fermi level cuts the bottom of the conduction band and there exists an electron pocket at the X point. Meanwhile, the top of the valence band touches the Fermi level at the Γ point. It is clear that the overlap between the majority valence band and the conduction band is small, which leads to the low-DOS region around E_F in the majority DOS as can be seen in Fig. 1. In the minority band, in which E_F is located in an energy gap of 0.41 eV, the situation is quite different. The Fermi level lies above the minority spin valence band maximum (VBM), which is the minimum energy required to flip a minority spin electron from the VBM to the majority spin Fermi level and is often referred to as the "spin-flip gap" [21]. In Mn_2Sn, the VBM gap is 0.24 eV. All this leads to 100% spin polarization in Mn_2Sn at the equilibrium lattice parameter.

As the lattice parameter decreases, Mn_2Sn gradually presents a semimetallic character in its spin bands. In the band structure of semimetal, two distinct energy bands overlap slightly with the Fermi level. In Fig. 2, as an example, the results for 5.5 Å are shown. In the majority band, the change is not quite clear. There exists a hole pocket at the Γ point and an electron pocket at the X point, which is due to the small shift of the majority band to higher energy with respect to the Fermi level. Meanwhile, it can be noticed that upon contraction of the lattice, the top of the valence band also touches the Fermi level at the W point, reflecting the enhanced d–d hybridization between Mn d states. The change is clearer in the minority spin band which is shifted to lower energy as the lattice parameter decreases. The bottom of the conduction band and the top of the valence band touch E_F at the X and the W point, respectively, which closes the half-metallic gap and makes Mn_2Sn a semimetal with compensated ferrimagnetic structure.

Increase of the lattice parameter has opposite effects. The majority conduction band moves to lower energy and overlaps with the Fermi level around the X point whereas the minority band shifts to higher energy and opens a gap of 0.8 eV with the top of the valence band touching the Fermi level at the Γ point.

The changes of the energy bands discussed above can be related to charge transfer between the spin-up and spin-down bands during the lattice contraction of expansion [22]. In Fig. 2, we can see that, with changing lattice parameters or applying strain we can control the energy gap around E_F as well as the carrier density of Mn_2Sn.

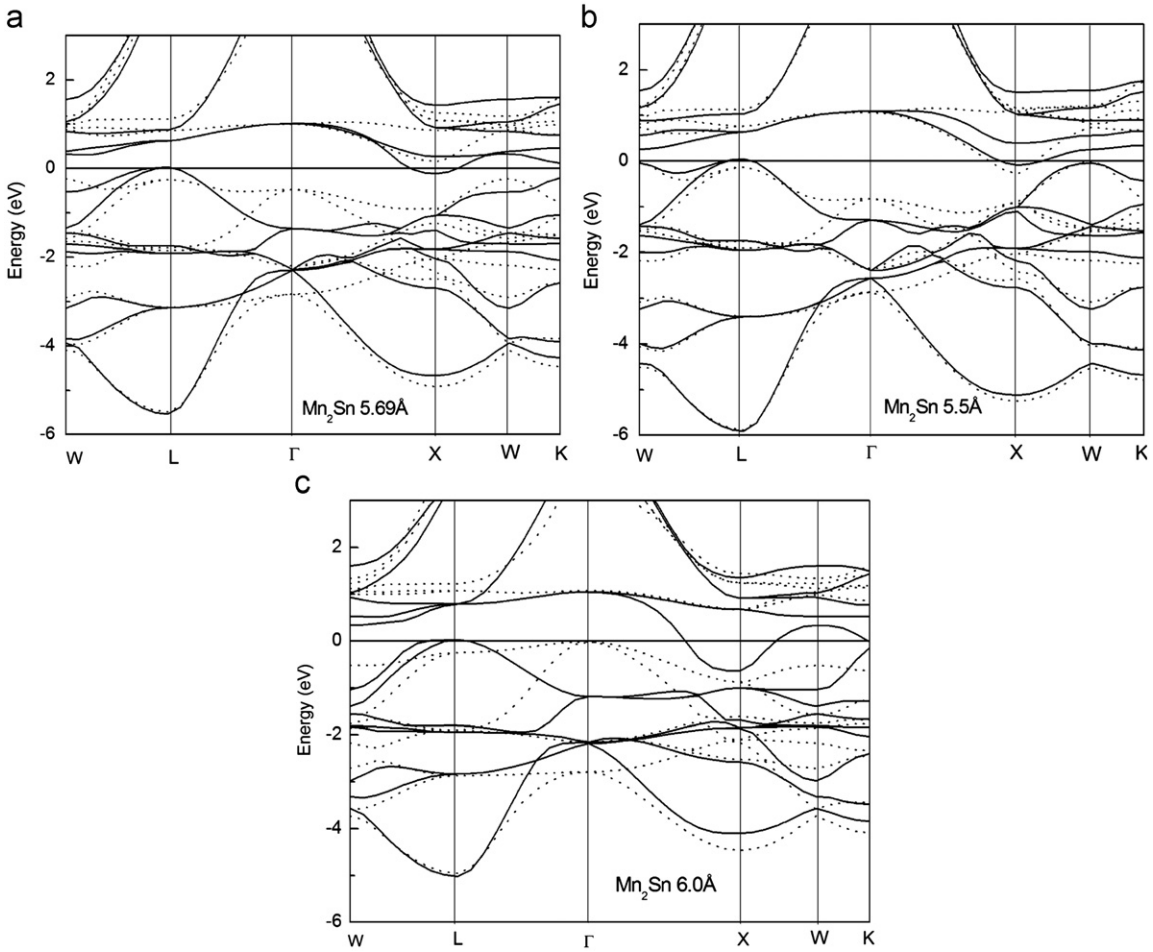

Fig. 2. Band structure of Mn_2Sn in the vicinity of the Fermi level for different lattice parameters: (a) at the calculated equilibrium lattice parameter 5.69 Å; (b) at a lattice parameter decreased by 3.3% (5.50 Å) and (c) at a lattice parameter increased by 5.4% (6.00 Å). The solid and dotted lines represent the majority and minority spin states, respectively.

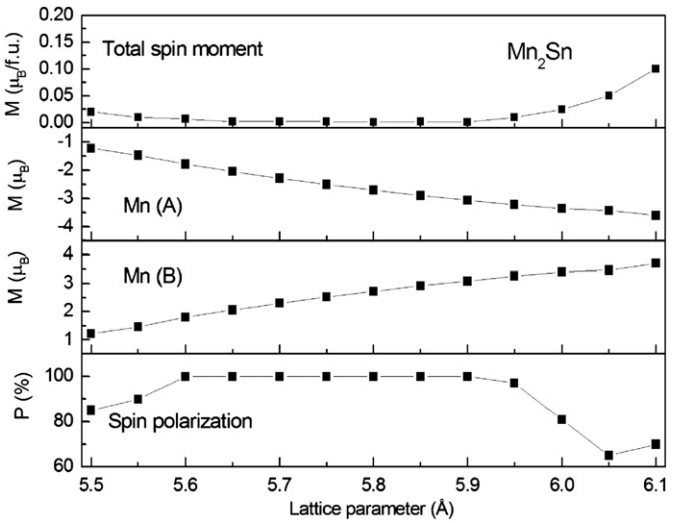

Fig. 3. Calculated total and partial spin moments and spin polarization ratios for Mn_2Sn as a function of the lattice parameter.

The changes of the total and partial spin moments of Mn_2Sn upon lattice distortion are presented in Fig. 3 in steps of 0.05 Å. The total spin moment M_t is quite stable within the range 5.60 Å–5.95 Å. It is always smaller than $0.01\mu_B$/f.u., indicating the completely compensated ferrimagnetic nature. This is because the Fermi level basically moves within the minority gap. However, the partial spin moments of Mn at the two different crystallographic sites are quite sensitive to the value of the lattice parameter. The absolute values of Mn (B) and Mn (A) moments increase monotonously if the lattice expands. The same has been observed in the Heusler alloys Co_2MnX (X=Si, Ge, Sn) [23] and Mn_2CuSb [24] and can be explained by the fact that, with increasing lattice parameter, the 3d localization is stronger and the Mn moment larger [9,20]. The moments of Mn (A) and Mn (B) have similar value but opposite sign. They compensate each other so that a nearly zero total moment is retained when the lattice parameter changes.

Finally, in order to establish to which extent the half-metallic properties are retained under lattice distortion, the spin polarization ratio P of Mn_2Sn is presented as a function of the lattice parameter in Fig. 3. The value of P is equal to $(N\uparrow - N\downarrow)/(N\uparrow + N\downarrow)$ where $N\uparrow$ and $N\downarrow$ are the majority and minority DOS at E_F, respectively. It can be seen that for Mn_2Sn a 100% spin polarization is obtained in a wide range from 5.6 Å to 5.9 Å, which is quite desired in technical applications such as thin-film systems. Here, it should be noted that, in the study of Fujii et al. [11], Mn_2Sn is only "close to" a half-metal as the minority gap around E_F in its DOS is a pseudogap. This is different from our results. The reason for this can be related to the larger lattice parameter in Ref. [11]. As discussed above, for $a=6.0$ Å, the top of the minority valence band will touch the Fermi level and affect the half-metallicity. So the influence of different calculation methods on the properties of Mn_2Sn is worth investigating further.

4. Conclusions

Ab initio calculations have been performed to investigate the electronic structure and magnetism of Mn_2Sn with half-Heusler structure. At the equilibrium lattice parameter 5.69 Å, Mn_2Sn is predicted to be a half-metallic fully compensated ferrimagnet (half-metallic antiferromagnet) with zero total spin moment. Mn_2Sn has 18 valence electrons and zero moment, which is mainly due to the antiparallel configuration of the Mn (A) and Mn (B) spin moments, which agrees well with the Slater–Pauling curve. The half-metallicity of Mn_2Sn is stable for a wide lattice-parameter range from 5.6 Å to 5.9 Å. Upon contraction of the lattice, a transition from half-metallic to semimetallic is observed.

Acknowledgment

This work is supported by National Natural Science Foundation of China in Grant nos. 50901028 and 50971130.

References

[1] R.A. de Groot, F.M. Mueller, P.G. van Engen, K.H.J. Buschow, Phys. Rev. Lett. 50 (1983) 2024.
[2] I. Zutic, J. Fabian, S. Das Sarma, Rev. Mod. Phys. 76 (2004) 323.
[3] C. Felser, G.H. Fecher, B. Balke, Angew. Chem. Int. Ed. 46 (2007) 668.
[4] I. Galanakis, P.H. Dederichs, N. Papanikolaou, Phys. Rev. B 66 (2002) 174429.
[5] H. van Leuken, R.A. de Groot, Phys. Rev. Lett. 74 (1995) 1171.
[6] S. Wurmehl, H.C. Kandpal, G.H. Fecher, C. Felser, J. Phys.: Condens. Matter 18 (2006) 6171.
[7] I. Galanakis, K. Özdoğan, E. Şaşıoğlu, B. Aktaş, Phys. Rev. B 75 (2007) 172405.
[8] H.Z. Luo, L. Ma, Z.Y. Zhu, G.H. Wu, H.Y. Liu, J.P. Qu, Y.X. Li, Physica B 403 (2008) 1797.
[9] I. Galanakis, K. Özdoğan, E. Şaşıoğlu, B. Aktaş, Phys. Rev. B 75 (2007) 092407.
[10] H. Okamto, J. Phase Equil. 20 (1999) 542.
[11] S. Fujii, S. Ishida, S. Asano, J. Phys. Soc. Jpn. 79 (2010) 124702.
[12] M.C. Payne, M.P. Teter, D.C. Allan, T.A. Arias, J.D. Joannopoolous, Rev. Mod. Phys. 64 (1992) 1065.
[13] M.D. Segall, P.L.D. Lindan, M.J. Probert, C.J. Pickard, P.J. Hasnip, S.J. Clark, M.C. Payne, J. Phys.: Condens. Matter 14 (2002) 2717.
[14] D. Vanderbilt, Phys. Rev. B 41 (1990) 7892.
[15] S.H. Vosko, L. Wilk, M. Nusair, Can. J. Phys. 58 (1980) 1200.
[16] J.P. Perdew, A. Zunger, Phys. Rev. B 23 (1981) 5048.
[17] S. Ogut, K.M. Rabe, Phys. Rev. B 51 (1995) 10443.
[18] B.R.K. Nanda, I. Dasgupta, J. Phys.: Condens. Matter 15 (2003) 7307.
[19] A. van de Walle, G. Ceder, Phys. Rev. B 59 (1999) 14992.
[20] I. Galanakis, Ph. Mavropoulos, P.H. Dederichs, J. Phys. D 39 (2006) 765.
[21] K. Capelle, G. Vignale, Phys. Rev. Lett. 86 (2001) 5546.
[22] H.C. Kandpal, G.H. Fecher, C. Felesr, G. Schonhense, Phys. Rev. B 73 (2006) 094422.
[23] S. Picozzi, A. Continenza, A.J. Freeman, Phys. Rev. B 66 (2002) 094421.
[24] X.P. Wei, J.B. Deng, S.B. Chu, G.Y. Mao, L.B. Hu, M.K. Yang, X.R. Hu, Comput. Mater. Sci. 50 (2011) 1175.